2008 IEEE International Conference on
Robotics and Automation
Pasadena, CA, USA, May 19-23, 2008

C-SAM: Multi-Robot SLAM using Square Root Information Smoothing

Lars A. A. Andersson and Jonas Nygårds

Abstract— **This paper presents Collaborative Smoothing and Mapping (C-SAM) as a viable approach to the multi-robot map-alignment problem. This method enables a team of robots to build joint maps with or without initial knowledge of their relative poses. To accomplish the Simultaneous Localization and Mapping this method uses Square Root Information Smoothing (SRIS). In contrast to traditional Extended Kalman Filter (EKF) methods the smoothing does not exclude any information and is therefore also better equipped to deal with non-linear process and measurement models. The method proposed does not require the collaborative robots to have initial correspondence. The key contribution of this work is an optimal smoothing algorithm for merging maps that are created by different robots independently or in groups. The method not only joins maps from different robots, it also recovers the complete robot trajectory for each robot involved in the map joining. It is also shown how data association between duplicate features is done and how this reduces uncertainty in the complete map. Two simulated scenarios are presented where the C-SAM algorithm is applied on two individually created maps. One basically joins two maps resulting in a large map while the other shows a scenario where sensor extension is carried out.**

I. Introduction

By solving the Collaborative Simultaneous Localization and Mapping (C-SLAM) problem it is possible to collect information about an environment faster and more accurately. The basic idea is to use multiple robots each making individual maps of an area. Map information is then exchanged as the robots communicate. The approach will work for two or more robots although the two-robot case is discussed in this work. The proposed method for C-SLAM uses Simultaneous *Smoothing and Mapping* (SAM) based on matrix square roots. This method was initially introduced in [1] and is later referred to as $\sqrt{SAM}$.

For two robots to have use of each other´s map information it is necessary for them to be highly correlated. This is done by having the robots make relative pose observations. These are later referred to as *rendezvous-measurements*. These measurements together with the trajectory for each robot during the measurements are then used to find a *connector* to align the individual maps. Since the connector represents the relation between two maps, the map joining itself does not spoil the sparsity of each submap. In the case of many robots working together there will be a number of connectors. The presented approach does not require the *rendezvous-measurements* to be done in both ways. It is enough to have one robot measuring the other.

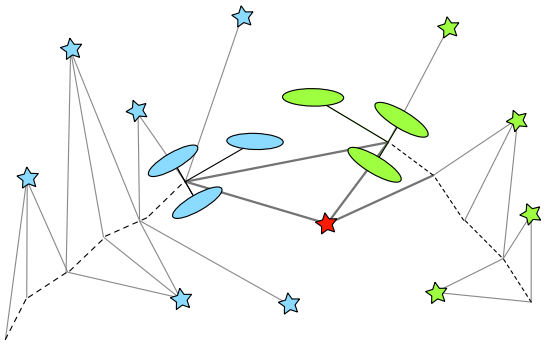

Fig. 1. Two robots rendezvous after exploration. The individually created maps are shared and joined into one single map. The new map information is then used as a priori information as exploration continues.

The approach presented here has similarities to the idea of Tectonic SAM (T-SAM) for a single robot [2]. However, there are some major differences in the usage. T-SAM is a divide-and-conquer approach used to partition a single robot´s map into sub-maps that are already aligned. In Collaborative SAM (C-SAM) the opposite is carried out, where each local map can be seen as a sub-map in the joint environment of two or more robots.

Since SRIS optimizes and recoverers the entire robot trajectory, this is used together with *rendezvous-measurements* to initiate a map alignment. This is especially important for the robustness of the map joining for robots with unknown initial correspondence since the success of the map joining is heavily dependent on how well the initiation is made. It is also helpful for eliminating spurious sensor information in noisy environments to increase the robustness of the result. Since the smoothing of the trajectory is part of the system there is no additional effort required for robots to share their past trajectories with each other, assuming bandwidth is an infinite resource. This can be very useful for trajectory planning in environments where not all obstacles are represented as map features, typically outdoors where a feature-free path is not necessarily free for travel.

The approach to information sharing presented in this work is also well suited for situations where bandwidth is a limited resource. For doing a map alignment the robots do not necessary have to share all the map information but only the poses and measurements related to the rendezvous. Since the map alignment is a basic requirement for joining two maps one can at an early stage decide not to share any more information if this first step does not succeed.

L. A. A. Andersson are with Department of Management and Engineering, Linköping University, S-581 83 Linköping, Sweden. robotics@ikp.liu.se

J. Nygårds are with Div. of Command and Control Systems, Swedish Defence Research Agency, S-581 11 Linköping, Sweden. jonny@foi.se

Two simulated scenarios show the effect and usefulness of the C-SAM. In the first scenario two robots explore an area individually. The maps from the two robots are joined using C-SAM, resulting in a large map with significantly lower uncertainty of the mapped features. The second scenario shows the effect of sensor extension. The idea is to have two robots explore an unknown environment while one of the robots is observing the other at all time. By doing this the range of the sensors can be extended to almost the double while drastically reducing the uncertainty of the features mapped furthest away.

It is important to note that this work is not about how well the $\sqrt{SAM}$ performs in general or how the computational cost can be affected by algebraic rework. We investigate how this framework can be used for fusing information between different members of a robot team and show how the smoothing can be effective in recovering errors accumulated over time.

II. Related Work

In recent years SLAM has come to be a well-studied problem. It was originally introduced in [3] and early results can be found in [4]. There are many different approaches used when it comes to performing SLAM. Some use traditional Bayesian estimation methods while others use non-Bayesian, such as Maximum Likelihood (ML), [5]. However, the most commonly used methods are Marcov localization using Particle Filter or various Kalman Filtering techniques. There have been several applications of this technology in a number of different environments, such as indoors, [6] underwater [7] and outdoors [4].

There are also some approaches for how to perform SLAM with multiple robots. Some use online collaboration [8] [9] [10] while others work with off-line data. An outdoor approach for distributed localization of a robot team is presented in [11]. This work also includes the use of the robot team for outdoor terrain mapping. An analytical expression for upper bounds of uncertainty for Cooperative Simultaneous Localization and Mapping (C-SLAM) has recently been derived [12].

A similar problem to what is discussed in this paper is presented in [13]. In contrast to the $\sqrt{SAM}$ approach an EKF based solution is presented. Another difference is that in our solution the *rendezvous-measurement* is handled separately from each robot, not requiring the measurements to be time synchronized or done in both ways. One problem with the EKF solution may be issues with the consistency of the map. Therefore, the EKF approach may not be suitable in all situations. This problem is brought up in [14], where it is shown that when dealing with large maps the EKF based SLAM algorithm has a tendency to diverge. It is stated that approximations and linearizations of system and measurement models cause the EKF to diverge [15]. It is shown that linearizaton errors lead to inconsistent estimates well before computational problems arise. However, a new robocentric method is proposed to reduce this effect.

In [1] a different approach for performing SLAM is proposed. This work investigates whether SRIS is a viable alternative to the EKF for solving the SLAM problem. It is stated that the SRIS approach is fundamentally better for these types of problems than the commonly used EKF. In contrast to traditional EKF methods, the smoothing does not exclude any information and is therefore also better equipped to deal with non-linear process and measurement models.

Recently, much effort has been put into making the $\sqrt{SAM}$ algorithm more efficient. In [16] a fast incremental version is presented. It is shown how an environment can be mapped in linear time and also how to obtain uncertainties needed for data association. An Out-of-Core, Submap-based approach is presented in [2]. This presents a method for large environment mapping in realtime by dividing the map into smaller maps, each linearized at a local reference. The local linearization can later be reused for back substitution in the entire map.

III. Smoothing and Mapping

Instead of looking at a filter approach we investigate the use of smoothing. The approach is to represent the SLAM problem as a belief net, initially introduced in [1]. The problem is described as finding the maximum a posteriori (MAP) estimate for an entire trajectory $\mathbf{X} = \{\mathbf{x}_i\}$ and the map $\mathbf{L} = \{\mathbf{l}_j\}$, given the observations $\mathbf{Z} = \{\mathbf{z}_k\}$ and the control inputs $\mathbf{U} = \{\mathbf{u}_i\}$. This is done by solving the following non-linear least-squares problem:

$$\{\mathbf{X},\mathbf{L}\}^* = \underset{\{\mathbf{X},\mathbf{L}\}}{argmin} \left\{ \sum_{i=1}^{M} \|f_i(\mathbf{x}_{i-1},\mathbf{u}_i) - \mathbf{x}_i\|^2_{\mathbf{\Lambda}_i} + \sum_{k=1}^{K} \|h_k(\mathbf{x}_{i_k},\mathbf{l}_{j_k}) - \mathbf{z}_k\|^2_{\mathbf{\Sigma}_k} \right\} \quad (1)$$

where $\|e\|^2_\Sigma = e^T\Sigma^{-1}e$ is defined as the Mahalanobis distance, given a covariance matrix Σ. By combining the Jacobians of the goal function into a matrix $\mathbf{A}$ and the prediction errors $\mathbf{a}_i \triangleq \mathbf{x}_i^0 - f_i(\mathbf{x}_{i-1}^0,\mathbf{u}_i)$ and $\mathbf{c}_k \triangleq \mathbf{z}_k - h_k(\mathbf{x}_{i_k}^0,\mathbf{l}_{j_k}^0)$ into the right hand side (RHS) vector $\mathbf{b}$, we obtain the following least squares problem:

$$\delta^* = argmin \|\mathbf{A}\delta - \mathbf{b}\|_2^2 \quad (2)$$

For more information about the background and calculation cost of $\sqrt{SAM}$ we refer the reader to [1].

As this work is presented in 2D/3DOF, the robot states $\mathbf{x}_i$ observations $\mathbf{z}_k$ and features $\mathbf{l}_j$ are represented as:

$$\mathbf{x}_i = \begin{bmatrix} x_i \\ y_i \\ \phi_i \end{bmatrix}, \mathbf{l}_j = \begin{bmatrix} x_j \\ y_j \end{bmatrix}, \mathbf{z}_k = \begin{bmatrix} x_k \\ y_k \end{bmatrix} \quad (3)$$

The features are seen as 2D point objects and are therefore only represented by two parameters. The robot observes a relative position between the robot and a feature. The observation is therefore also represented by a 2D vector.

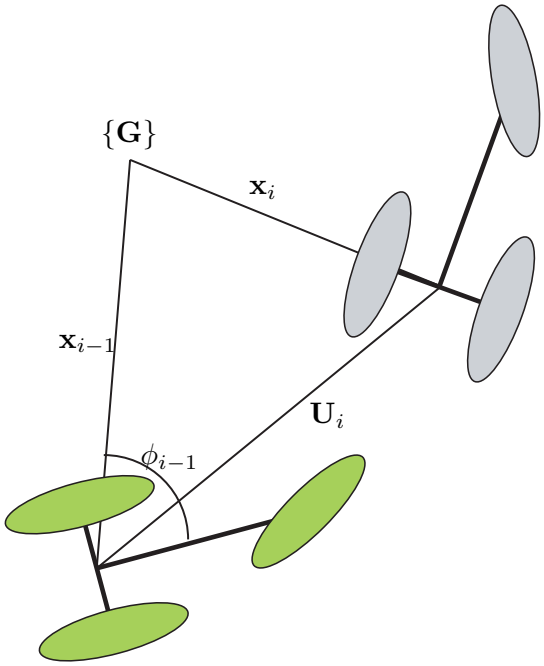

Fig. 2. A robot moving between two poses over a period of time T. From this an exact discrete kinematic model is derived.

A. Motion Model

A discrete constant turn model with lateral slip is used for describing the motion of each robot. The system is driven by the translational v_i, v_{lat_i} and rotational ω_i speeds:

$$\mathbf{u}_i = \begin{bmatrix} v_i \\ v_{lat_i} \\ \omega_i \end{bmatrix}, \mathbf{w}_i = \begin{bmatrix} \tilde{v}_i \\ \tilde{v}_{lat_i} \\ \tilde{\omega}_i \end{bmatrix} \tag{4}$$

where $\mathbf{u}_i$ is the driving vector. It is assumed that the error vector for the driving parameters, $\mathbf{w}_i$, is normally distributed and zero-mean with standard deviation σ_{v_i}, $\sigma_{v_{lat_i}}$ and σ_{ω_i} respectively.

The non-linear transition function $f_i(.)$ from (1) is the process model used to describe the change between two consecutive poses, $\mathbf{x}_{i-1} \rightarrow \mathbf{x}_i$, in the coordinate reference frame $\{\mathbf{G}\}$, see Figure 2. The pose change is a function of the driving parameter $\mathbf{u}_i$ and the corresponding noise $\mathbf{w}_i$.

$$\begin{aligned} \mathbf{x}_i &= f(\mathbf{x}_{i-1}, \mathbf{u}_i + \mathbf{w}_i) \\ f(\mathbf{x}_{i-1}, \mathbf{u}_i) &= \mathbf{x}_{i-1} + \mathbf{R}(\phi_{i-1})\mathbf{U}_i \end{aligned} \tag{5}$$

where

$$\mathbf{R}(\phi_i) = \begin{bmatrix} \cos(\phi_i) & -\sin(\phi_i) & 0 \\ \sin(\phi_i) & \cos(\phi_i) & 0 \\ 0 & 0 & 1 \end{bmatrix} \tag{6}$$

In (5) the change of pose from robot local coordinates at $\mathbf{x}_{i-1}$ is represented by a vector $\mathbf{U}_i$. Instead of approximating the discrete model from a continuum, this pose change is extracted using geometric reasoning from Figure 2. The pose change $\mathbf{U}_i$ of the platform during a sample T then becomes:

$$\mathbf{U}_i = \begin{bmatrix} \frac{v_i}{\omega_i}\sin(\omega_i T) - \frac{v_{lat_i}}{\omega_i}(1-\cos(\omega_i T)) \\ \frac{v_i}{\omega_i}(1-\cos(\omega_i T)) + \frac{v_{lat_i}}{\omega_i}\sin(\omega_i T) \\ \omega_i T \end{bmatrix} \tag{7}$$

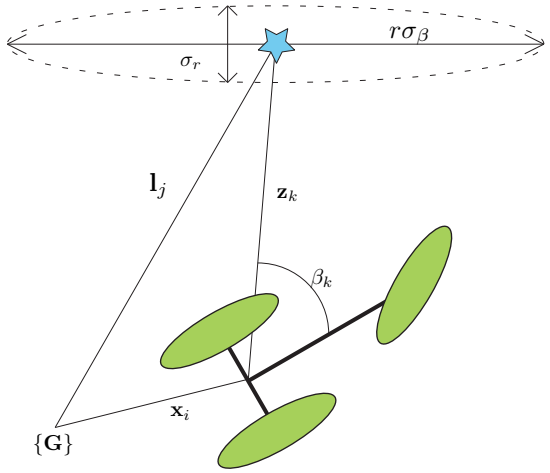

Fig. 3. A single measurement between a robot and a feature. The parameters are the same for measurement between two robots.

For prediction of the robot motion the nonlinear transition function is used. It should be noted that this function is exact, and not approximative, for all sample times T, as long as $\mathbf{u}_i$ is constant over the sample. The error transformation is done using a first order Taylor expansion. Due to robot kinematics, the lateral velocity is not controllable in this case and is therefore set to zero ($v_{lat_i} = 0$); however, the lateral slip error is still present and therefore this term can not be eliminated before the Jacobians are calculated. The linearized transition function (5) then becomes:

$$\begin{aligned} \mathbf{x}_i &= \hat{\mathbf{x}}_i + \tilde{\mathbf{x}}_i \\ \hat{\mathbf{x}}_i &= f(\hat{\mathbf{x}}_{i-1}, \mathbf{u}_i) \end{aligned} \tag{8}$$

The first order Taylor series of the prediction error can be described as:

$$\tilde{\mathbf{x}}_i = \mathbf{F}_i^{i-1}\tilde{\mathbf{x}}_{i-1} + \mathbf{G}_i^{i-1}\mathbf{w}_i \tag{9}$$

where $\mathbf{F}_{i+1}^i$ and $\mathbf{G}_{i+1}^i$ are the Jacobians of $f(.)$ evaluated at $\hat{\mathbf{x}}_i$ and $\mathbf{u}_i$ respectively. The covariance for the motion between two consecutive poses then becomes:

$$\mathbf{\Lambda}_i = \mathbf{G}_i^{i-1}\begin{bmatrix} \sigma_v^2 & 0 & 0 \\ 0 & \sigma_{v_{lat}}^2 & 0 \\ 0 & 0 & \sigma_\omega^2 \end{bmatrix}\mathbf{G}_i^{T\,i-1} \tag{10}$$

B. Sensor Model

The sensor used in this work makes measurements in polar coordinates. Typical sensors with these characteristics are laser range scanners and cameras. The work also applies to other sensor types. In such cases the sensor model will be different. Since the robot map uses cartesian coordinates the actual measurement is transformed into an observation. This scale better in cases when multiple sensors are mounted on the robot since the framework only needs to handle the observation model and not all different sensor models.

The measured variables are range, r_k, and bearing, β_k, from the robot origin to the observed feature.

$$\begin{aligned} r_k &= \hat{r}_k + \tilde{r}_k \\ \beta_k &= \hat{\beta}_k + \tilde{\beta}_k \end{aligned} \tag{11}$$

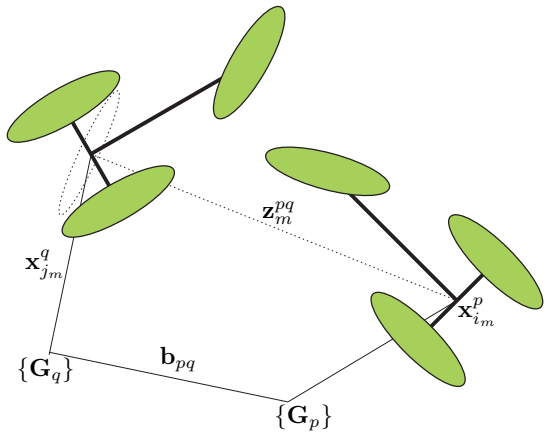

Fig. 4. The two robots each have a local coordinate system G. The base node bp_q represents the link between the two maps.

We assume the measurement errors, $\tilde{r}_k$ and $\tilde{\beta}_k$, to be normally distributed and zero-mean with standard deviation σ_{r_k} and σ_{β_k} respectively. In Figure 3 all of the variables involved in a polar measurement are presented. From the measured variables in (11) an observation $\mathbf{z}_k$ is generated.

$$\mathbf{z}_k = \begin{bmatrix} r_k \cos(\beta_k) \\ r_k \sin(\beta_k) \end{bmatrix} \tag{12}$$

The observation is modelled as a function $h_k(.)$ of the robot pose when the measurement is done and the estimated feature position is

$$\mathbf{z}_k = h_k(\mathbf{x}_{i_k}, \mathbf{l}_{j_k}) + \mathbf{v}_k \tag{13}$$

where the prediction error $\mathbf{v}_k$ is approximated as normally distributed zero-mean measurement noise with corresponding covariance $\mathbf{\Sigma}_k$:

$$\mathbf{\Sigma}_k = \mathbf{R}(\beta_k) \begin{bmatrix} {\sigma_{r_k}}^2 & 0 \\ 0 & r_k^2 {\sigma_{\beta_k}}^2 \end{bmatrix} \mathbf{R}(\beta_k) \tag{14}$$

where

$$\mathbf{R}(\beta_k) = \begin{bmatrix} \cos(\beta_k) & -\sin(\beta_k) \\ \sin(\beta_k) & \cos(\beta_k) \end{bmatrix} \tag{15}$$

From Figure 3 it is possible to obtain the observation model in a way similar to how the measurement model (12) is constructed:

$$h_k(\mathbf{x}_{i_k}, \mathbf{l}_{j_k}) = \mathbf{R}(\phi_{i_k})^{-1} (\mathbf{l}_{j_k} - \begin{bmatrix} x_{i_k} & y_{i_k} \end{bmatrix}^T) \tag{16}$$

where $\mathbf{R}(\phi_{i_k})$ is the same type of rotational matrix as (15). The linearized observation model then becomes

$$h_k(\mathbf{x}_{i_k}, \mathbf{l}_{j_k}) \approx h_k(\hat{\mathbf{x}}_{i_k}, \hat{\mathbf{l}}_{j_k}) + \mathbf{H}_k^{i_k} \tilde{\mathbf{x}}_{i_k} + \mathbf{J}_k^{j_k} \tilde{\mathbf{l}}_{j_k} \tag{17}$$

where $\mathbf{H}_k^{i_k}$ and $\mathbf{J}_k^{j_k}$ are the Jacobians of $h_k(.)$ evaluated at $\mathbf{x}_{i_k}$ and $\mathbf{l}_{j_k}$ respectively.

IV. Collaborative SAM

As stated earlier, this work is about presenting a method for sharing map information between members of a robot team. Without loss of generality we will from this point on discuss the map alignment and joining between two robots. Each robot p, q has its own map represented in the local coordinate frames $\{G_p\}$ and $\{G_q\}$ respectively, see Figure 4. Before any map information is shared it needs to be locally optimized by solving (2) for all nodes related to the respective robot. This enables us to distribute the optimization needed for map alignment and eliminate duplicate features. The map alignment is solved by creating a *base node* that connects the local coordinate frames of the maps to be joined. For this to work properly it is assumed that each of the two maps is adequately linearized. One way of ensuring good linearization is to work with smaller maps. Since we are working with rather small maps it is possible to recover the complete covariance for the entire map when doing the data association. However, this is not necessary if computer resources become a problem. In [16] it is shown how the information necessary for performing data association is extracted in realtime. Our approach is also well suited for later incorporation of the T-SAM algorithm [2], since the T-SAM has the possibility to work with small submaps linearized locally.

A. Map Alignment

Algorithm 1: Solving basenode

Optimize local robot maps separately
Add rendezvous-measurements to RHS vector $\mathbf{b}$ and $\mathbf{A}$' with (22) and (23) respectively
while $norm(\mathbf{b}) > limit$ **do**
  Solve (2) for $\mathbf{A}$'
  Re-linearize nodes in $\mathbf{b}$ and $\mathbf{A}$' added by (22) and (23)
end

The map alignment is based on a *rendezvous* between the two robots. The *rendezvous* is basically a set of poses for two robots together with a set of observations between the robots over the same poses. These observations will later be referred to as the *rendezvous-measurements*. It is important to note that these measurements do not necessary have to be in both directions. The association of the *rendezvous-poses* with the *rendezvous-measurements* is solved by assuming the two robots are time-synchronized and it is thereby possible to associate the observation to the pose of each robot using a time stamp. *Rendezvous-measurements* are range and bearing modelled in the same way as described in (12). Since the information in the *rendezvous-measurements* spans over both robot maps, a new set of constraints is added, referred to as the *connector*.

For the alignment a common reference between the two maps is needed. A new state, or *base node*, is therefore introduced in the system. This node, $\mathbf{b}_{pq}$, is used for describing the mapped nodes in $\{\mathbf{G}_q\}$ in the frame of $\{\mathbf{G}_p\}$. The *base node* can easily be transformed to the inverse relationship by using compounding from [3]:

$$\mathbf{b}_{qp} = \ominus \mathbf{b}_{pq} \tag{18}$$

The initiation of $\mathbf{b}_{pq}$ is done by using the first observation between the robots, transformed over the poses for the

observation:

$$\mathbf{b}_{pq}^{0} = \mathbf{x}_{i_m}^{p} \oplus (\mathbf{z}_{m}^{pq} \oplus (\ominus \mathbf{x}_{j_m}^{q})) \tag{19}$$

where $\mathbf{z}_m^{pq}$, are the *rendezvous measurements* used for aligning the two maps, while $\mathbf{x}_{i_m}^{p}$ and $\mathbf{x}_{j_m}^{q}$ are the *rendezvous poses*. An additional optimization constraint is added to the goal function (1) for handling these new observations:

$$\sum_{m=1}^{N} \left\| c_m(\mathbf{x}_{i_m}^{p}, \mathbf{b}_{pq}, \mathbf{x}_{j_m}^{q}) - \mathbf{z}_{m}^{pq} \right\|_{\Sigma_m}^{2} \tag{20}$$

The final goal function for the complete system when aligning the maps then becomes:

$$\begin{aligned} \{\mathbf{X}, \mathbf{L}\}^{*} = \underset{\{\mathbf{X},\mathbf{L}\}}{argmin} \Bigg\{ & \sum_{i=1}^{M} \left\| f_i(\mathbf{x}_{i-1}, \mathbf{u}_i) - \mathbf{x}_i \right\|_{\mathbf{\Lambda}_i}^{2} \\ & + \sum_{k=1}^{K} \left\| h_k(\mathbf{x}_{i_k}, \mathbf{l}_{j_k}) - \mathbf{z}_k \right\|_{\mathbf{\Sigma}_k}^{2} \\ & + \sum_{m=1}^{N} \left\| c_m(\mathbf{x}_{i_m}^{p}, \mathbf{b}_{pq}, \mathbf{x}_{j_m}^{q}) - \mathbf{z}_{m}^{pq} \right\|_{\mathbf{\Sigma}_m}^{2} \Bigg\} \end{aligned} \tag{21}$$

where $c_m(.)$ is the observation model used for prediction of the base node:

$$c_m(\mathbf{x}_{i_m}^{p}, \mathbf{b}_{pq}, \mathbf{x}_{j_m}^{q}) = (\ominus \mathbf{x}_{i_m}^{p} \oplus \mathbf{b}_{pq}) \oplus \mathbf{x}_{j_m}^{q} \tag{22}$$

The prediction error for the observation, $\mathbf{n}_m$, then becomes:

$$\mathbf{n}_m \triangleq \mathbf{z}_{m}^{pq} - c_m(\mathbf{x}_{i}^{p}, \mathbf{b}_{pq}, \mathbf{x}_{j}^{q}) \tag{23}$$

The *connector*, $\mathbf{C}$, holds the information gained from each *rendezvous-measurement* and how this is related to the *base node*. Each row in the connector is typically:

$$\mathbf{C}_m = \begin{bmatrix} \mathbf{C}_{i_m}^{p} & \dots & \mathbf{C}_{j_m}^{q} & \dots & \mathbf{B}_{m}^{pq} \end{bmatrix} \tag{24}$$

where $\mathbf{C}_{i_m}^{p}$, $\mathbf{C}_{j_m}^{q}$ and $\mathbf{B}_{m}^{pq}$ are the corresponding Jacobians of (22) pre-multiplied with the observation covariance $\mathbf{\Sigma}_m$. The *connector* is evaluated for the robot poses when the *rendezvous-measurement* is done.

Since (20) spans over multiple robot maps it is necessary to create a Jacobian matrix to include all *rendezvous-measurements* and *rendezvous poses* from each robot into a complete system. The system also needs to include the *base node* as well. The new matrix of Jacobians then becomes:

$$\mathbf{A}' = \begin{bmatrix} \mathbf{A}_{m}^{p} & 0 & 0 \\ 0 & \mathbf{A_m}^{q} & 0 \\ \mathbf{C}_{m}^{p} & \mathbf{C}_{m}^{q} & \mathbf{B}_{m}^{pq} \end{bmatrix} \tag{25}$$

where $\mathbf{A}_m^p$ and $\mathbf{A}_m^q$ are the rendezvous subset of square root information matrices of each locally optimized map from the respective robot. It is worth mentioning that the robot submaps do not need to be transformed into the same reference frame for alignment. All states are kept in in the original linearization point when solving the *base node*. As the least squares equation (1) is solved for $\mathbf{A}'$ and the RHS $[\mathbf{a}_{i_m} \quad \mathbf{c}_{k_m} \quad \mathbf{n}_m]^T$ using Algorithm 1, the *base node* converges and the two maps are aligned. It should be noted that the initial value of $\mathbf{b}_{pq}$ will influence the number of iterations needed for convergence.

Algorithm 2: Feature association

```
Calculate the covariance as: P = (A'^T A')^{-1}
for l_j^p ∈ L^p do
    for l_j^q ∈ L^q do
        Compute the Mahalanobis distance D_ij
        with (26)
        if D_ij < ξ then
            Add a constraint for the match in A' using
            (22) and (23)
        end
    end
end
Solve (2) a final time with the recently added
association constraints.
```

B. Map Joining

When the initial estimate of $\mathbf{b}_{pq}$ is retrieved, the maps are aligned but may still be improved by associating features present in both maps. This is done by matching features from both maps to one another. Initially, one can consider only features that are observed during the rendezvous for association. These features are the ones most correlated to the poses where the map alignment is done and will therefore have the greatest impact on the result. Since a faulty match would have a considerable impact on the result it is important that the matching is done correctly. Therefore, all of these features are matched to one another by formulating a test based on the Mahalanobis distance. The hypothesis is that if two features are the same, the poses of the two features are the same; consequently, a relative observation, $\mathbf{z}_{ij}$, between them should be zero if the hypothesis is true.

$$\begin{aligned} \mathbf{z}_{ij} &= \mathbf{l}_{i}^{p} - \mathbf{l}_{j}^{q} = 0 \\ \hat{\mathbf{z}}_{ij} &= c_m(\mathbf{l}_{i}^{p}, \mathbf{b}_{pq}, \mathbf{l}_{j}^{q}) \\ \mathbf{r} &= \mathbf{z}_{ij} - \hat{\mathbf{z}}_{ij} = -c_m(\mathbf{l}_{i}^{p}, \mathbf{b}_{pq}, \mathbf{l}_{j}^{q}) \\ \mathbf{H} &= \begin{bmatrix} \dots & \mathbf{C}_{m_i}^{p} & \dots & \mathbf{C}_{m_j}^{q} & \dots & \mathbf{B}_{m}^{pq} \end{bmatrix} \\ \mathbf{P} &= (\mathbf{A}'^{T}\mathbf{A}')^{-1} \\ \mathbf{S} &= \mathbf{H}\mathbf{P}\mathbf{H}^{T} \\ D_{pq} &= \mathbf{r}^{T}\mathbf{S}^{-1}\mathbf{r} \end{aligned} \tag{26}$$

where D_{pq} is the Mahalanobis distance. If this is below the threshold ξ and the features are uniquely matched to each other then we assume the two features $\mathbf{l}_j^p$ and $\mathbf{l}_j^q$ to be the same feature. To incorporate this into the optimization this is added as a new row in the *connector* by evaluating (22) and (24) for the feature states $\mathbf{l}_i^p$ and $\mathbf{l}_j^q$ instead of robot poses. Algorithm 2 shows how the matching is done. Assuming the linearization point for the *base node* is adequate this is a single pass algorithm. Otherwise, it may require a few iterations. If computer resources permit, it one can also try to match other features in the maps. If the robots have had a rendezvous earlier and meet again after some time, it is possible to handle loop closing with the same approach as explained above.

V. Experimental results

This section describes two simulated experiments conducted in a synthetic environment. These are meant to show some of the benefits of C-SAM. Both experiments are based on two robots exploring an unknown environment. No a priori information is available and the two robots do not have any initial correspondence. Each robot is equipped with a simulated URG-04LX Scanning Laser Rangefinder mounted at the robot center. This scanner has a range of 4 meters and a 240 degree field of view. The angular resolution is 0.36^o while the range measurements are +/- 10mm. Based on this, our sensor noise characteristics are set to: $\sigma_{r_k} = 0.01$ and $\sigma_{\beta_k} = 0.012$. The two robots each make one laser scan for every pose.

A. Map Joining

The first experiment shows the benefits of map joining as a tool to increase the accuracy of one's own map as well as gain extended information about features outside the already explored area. Both robots have the scanning laser mounted viewing in the forward direction of the robot motion. The field of view for the laser scanner is 240 degrees. In Figure 5 one can see that the angular uncertainty increases in steps over the samples. This effect can be explained by the fact that our sensor only observes a feature position and not a complete pose. This causes the robot to rely heavily on the motion prediction in the case of not observing any features or only observing one feature and therefore continuously losing information for each new sample.

In figure 5 one can see the direct benefit from joining the maps of two robots making a *rendezvous* when meeting each other. Both of the robots clearly benefit from increased certainty about the estimates of both features and trajectory at the time of rendezvous and beyond. From the rendezvous point the uncertainty will stay below what can be achieved with only a single robot SAM since the minimal information gain from the rendezvous is the robots´ trajectories, which is used for reducing the angular uncertainty during the rendezvous. It should be noted that in the experiment the C-SAM manages to decrease the angular uncertainty for both robots in samples prior to the rendezvous as well. This effect can be explained by the fact that a number of features were associated correctly from both maps and the smoothing will to some extent recover this error backwards. However, the effect is heavily dependent on the environment and how well the robots manage to associate duplicate features in the two initial robot maps.

B. Sensor Extension

This experiment points out the benefits of using C-SAM as a tool for extending sensors and reducing process noise in a head-to-tail relationship. This is an example of two robots with different terrain capabilities working together. A typical example would be to have an observing robot moving on a tarmacked road surface, Robot-P, while the exploring robot, Robot-Q, is working in the terrain next to the road. In this experiment, Robot-P has relatively low process noise and observes Robot-Q and close features with the mounted URG range scanner. Robot-Q, with higher process noise, five times higher to be more exact, is exploring a rather feature-dense area and manages to observe features further away. The laser scanners are mounted centered in the robots´ forward direction with a 180-degree field of view for both laser scanners.

We can show that the resulting map for both robots is drastically enhanced. The exploring Robot-Q almost completely inherits the noise characteristics of the observing Robot-P, resulting in drastically better map information. In Figure 6 it is clear that both robots have great benefit of the C-SAM. Since robot-P observes robot-Q over the complete trajectory, both robots decrease their uncertainty in every sample, resulting in a more accurate map than if the two robots had operated individually.

VI. Conclusions

In this paper we have contributed an efficient and straightforward algorithm to align and join maps and trajectories in a multi-robot system. Since the algorithm not only joins the maps but also recovers the trajectory of the robots it is well suited for mission control, where the trajectory information can be reused by robots to verify a possible path in the newly discovered region. It is also shown how association between duplicate features is accomplished with the calculation of Mahalanobis distance. If a duplicate feature is successfully identified in the aligned map, the information is used by the smoother to tighten up the map and recover some uncertainty for both robots prior to the rendezvous.

We have found that the initiation of the *base node* is important for the convergence speed of the optimization. We believe that it may also effect the result of the final map. In future work we plan to investigate how the choice of base node affects system behavior. Since the effect of two robots exchanging map information is likely to cause the robots to enter recently explored areas, see section V-A, a natural extension of this work is to investigate how the same framework can be used to deal with loop closing for a single and multi-robot system.

In the future we will also investigate how the extracted trajectories can be used for more efficient path planning. It is reasonable to believe that a robot with information on how other robots have traveled can operate faster and will be more efficient.

References

[1] F. Dellaert and M. Kaess, "Square root sam simultaneous localization and mapping via square root information smoothing," *International Journal of Robotics Research*, vol. 25, pp. 1181–1203, 2006.

[2] K. Ni, D. Steedly, and F. Dellaert, "Tectonic sam: Exact, out-of-core, submap-based slam," in *Proceedings of International Conference on Robotics and Automation (ICRA 2007)*, 2007. [Online]. Available: http://www-static.cc.gatech.edu/ nikai/research/Ni07icra.pdf

[3] R. Smith, M. Self, and P. Cheesman, "Estimating uncertain spatial relationships in robotics," in *Proceedings of the 2nd Annual Conference on Uncertainty in Artificial Intelligence (UAI-86)*. New York, NY: Elsevier Science Publishing Comapny, Inc., 1986, pp. 435–461.

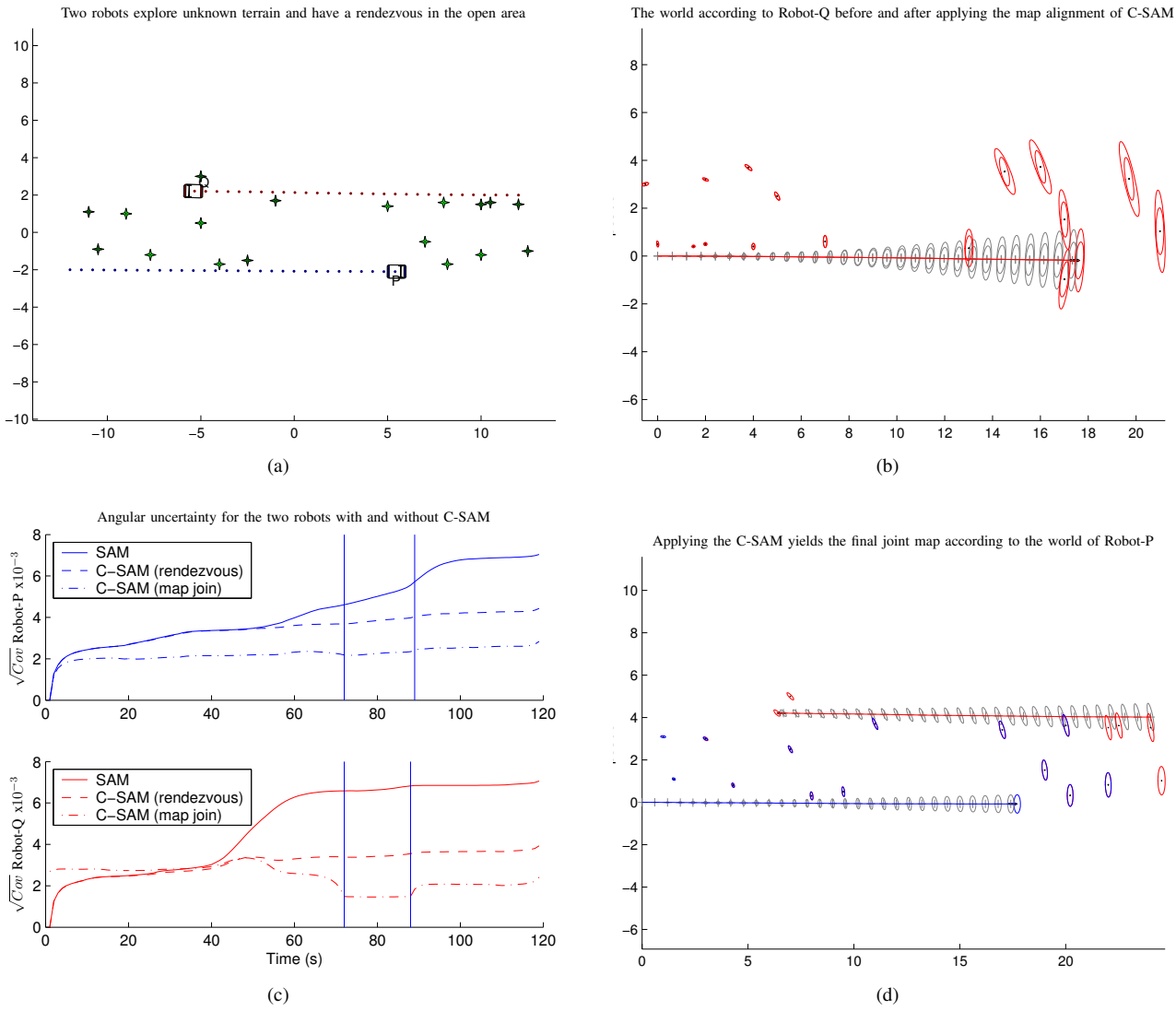

Fig. 5. (a) The scenario consists of two robots moving out of two feature-dense areas where the robots rendezvous in-between. Every fourth sample of the true poses for the trajectory is plotted with dots. (b) The regular $\sqrt{SAM}$ algorithm is applied onto Robot-Q's map. The resulting covariance for the trajectory and features before and after C-SAM is applied is shown. For clearer figures the ellipses are plotted with 18σ. (c) The angular uncertainty for both robot trajectories, before and after the C-SAM algorithm is applied. The two vertical lines indicate between what samples the rendezvous occurred. It is clear that C-SAM recoverers some uncertainty not only for the poses during the rendezvous but also before and after. The big step in uncertainty for Robot-Q starting at sample 40 is because all features fall out of range of the sensor while the robot needs to rely only on motion prediction. This effect is marginalized using C-SAM because sensor measurements from the complete scene are coupled over the *rendezvous-measurements*. (d) The final covariance of the joint map in the perspective of Robot-P's starting position.

[4] P. Moutarlier and R. Chatila, "An experimental system for incremental environment modelling by an autonomous mobile robot," in *Proceedings of The First International Symposium on Experimental Robotics*, Montreal, Canada, 1989, pp. 327–346.

[5] A. Howard, M. J. Matari´c, and G. S. Sukhatme, "Localization for mobile robot teams using maximum likelihood estimation," in *Proceedings of the IEEE/RSJ International Conference on Intelligent Robots and Systems*, EPFL, Switzerland, 2002.

[6] A. Makarenko, S. Williams, F. Bougault, and H. F. Durrant-Whyte, "An experiment in integrated exploration," in *Proceeding of IEEE/RSJ International Conference on Intelligent Robot Systems*, 2002.

[7] S. Williams, P. Newman, G. Dissanayake, and H. F. Durrant-Whyte, "Autonomous underwater simultaneous localization and map building," in *Proceedings of International Conference on Robotics and Automation (ICRA 2000)*, 2000.

[8] A. Howard, "Multi-robot simultaneous localization and mapping using particle filters," in *Proceedings of Robotics: Science and Systems (RSS)*, Jun 2005. [Online]. Available: http://www.roboticsproceedings.org/rss01/p27.pdf

[9] D. Fox, W. Burgard, H. Kruppa, and S. Thrun, "A probabilistic approach to collaborative multi-robot localization." *Autonomous Robots, Special Issue on Heterogeneous Multi-Robot Systems*, vol. 8, no. 3, pp. 325–344, 2000.

[10] S. Roumeliotis and G. Bekey, "Distributed multi-robot localization," *IEEE Transactions on Robotics and Automation*, vol. 18, no. 5, pp. 781–795, October 2002.

[11] R. Madhavan, K. Fregene, and L. E. Parker, "Terrain aided distributed heterogeneous multirobot localization and mapping," *Autonomous Robots*, vol. 17, no. 1, pp. 23–39, 2004.

[12] A. I. Mourikis and S. I. Roumeliotis, "Predicting the performance of cooperative simultaneous localization and mapping (c-slam)," *The International Journal of Robotics Research*, vol. 25, no. 12, pp. 1273–1286, 2006.

[13] X. S. Zhou and S. I. Roumeliotis, "Multi-robot slam with unknown initial correspondence: The robot rendezvous case," in *Proceedings of International Conference on Intelligent Robots and Systems, IROS*,

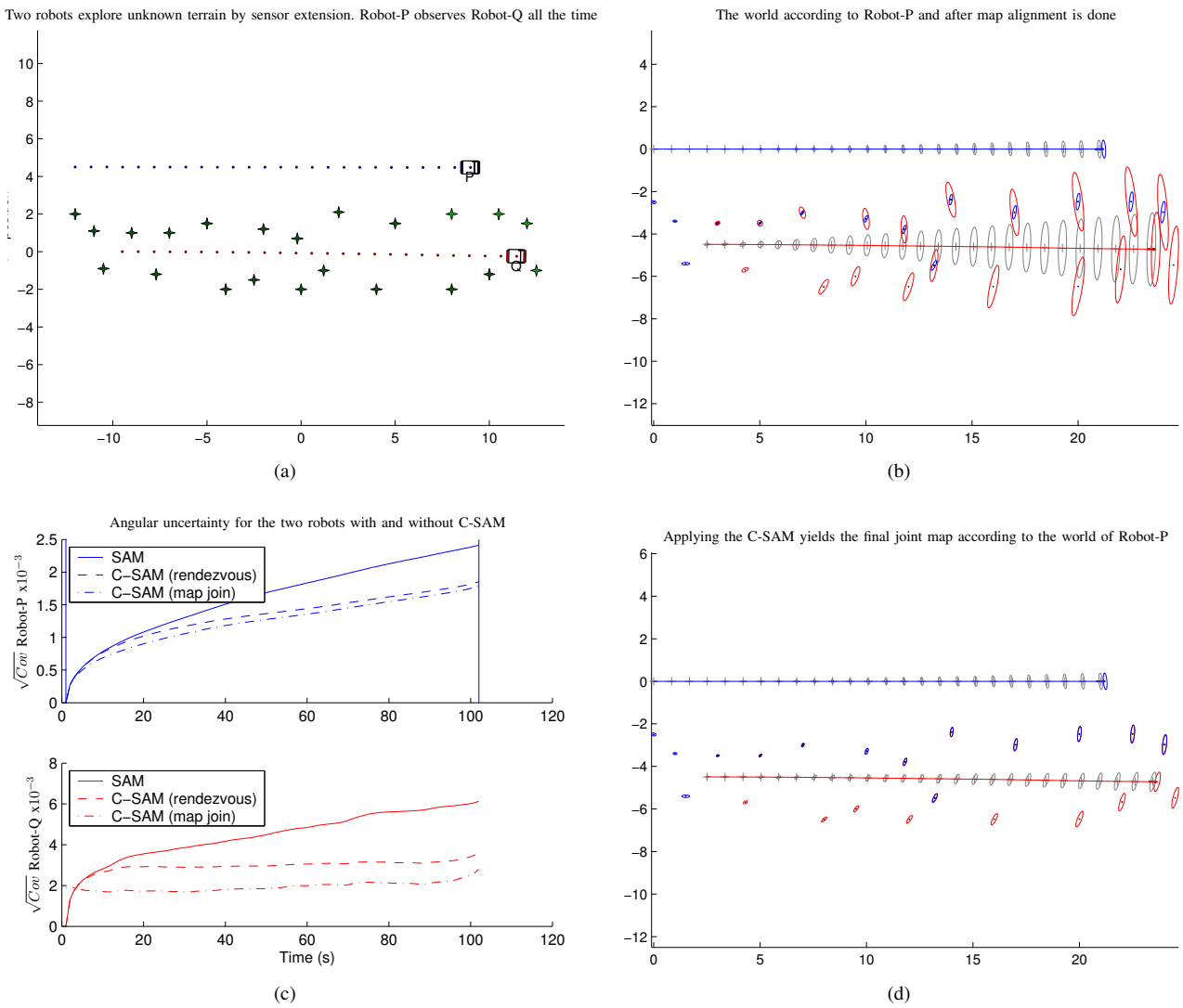

Fig. 6. (a) The scene in which the upper robot, Robot-P, has considerably lower process noise than the one below, Robot-Q. The rendezvous measurements consist only of measurements from Robot-P towards Robot-Q. Every fourth sample of the true poses for the trajectory is shown with dots. (b) The resulting map of both robots with C-SAM only using rendezvous measurements, represented in the reference frame of Robot-P. (c) The angular uncertainty over time for the two robots, before and after applying C-SAM. Note the drastic decrease in uncertainty for Robot-Q; it has almost inherited the uncertainty from Robot-P. (d) Final map in the perspective of Robot-P.

2006.

[14] J. A. Castellanos, J. Neira, and J. D. Tardós, "Limits to the consistency of ekf-based slam," in *Proceedings of Intelligent Autonomous Vehicles*. IFAC/EURON, July 2004.

[15] Y. Bar-Shalom and X. Li, *Estimation and Tracking: Principles, Techniques and Software*. Artech House, 1993, iSBN-10: 096483121X.

[16] M. Kaess, A. Ranganathan, and F. Dellaert, "Fast incremental square root information smoothing," in *Proceedings of International Joint Conference on Artificial Intelligence*, Hyderabad, India, January 2007.